

Numerical evaluation of induction heating assisted compaction technology for low temperature asphalt pavement construction

Zhou, Changhong; Liu, Xueyan; Apostolidis, Panos

Publication date

2017

Document Version

Accepted author manuscript

Published in

The 96th Annual Meeting of the Transportation Research Board

Citation (APA)

Zhou, C., Liu, X., & Apostolidis, P. (2017). Numerical evaluation of induction heating assisted compaction technology for low temperature asphalt pavement construction. In *The 96th Annual Meeting of the Transportation Research Board* Article 17-03165 Transportation Research Board (TRB).

Important note

To cite this publication, please use the final published version (if applicable).
Please check the document version above.

Copyright

Other than for strictly personal use, it is not permitted to download, forward or distribute the text or part of it, without the consent of the author(s) and/or copyright holder(s), unless the work is under an open content license such as Creative Commons.

Takedown policy

Please contact us and provide details if you believe this document breaches copyrights.
We will remove access to the work immediately and investigate your claim.

1 **Numerical evaluation of induction heating assisted compaction technology for low**
2 **temperature asphalt pavement construction**

5 **Changhong Zhou, Corresponding Author**

6 Dalian University of Technology
7 No. 2 Linggong Rd., Dalian, China, 116023
8 Tel: +86 18940836303; Email: czhou@dlut.edu.cn

10 Delft University of Technology
11 Stevinweg 1, Delft, The Netherlands, 2628 CN
12 Tel: +31 (0)626107910; Email: C.Zhou@tudelft.nl

14 **Xueyan Liu**

15 Delft University of Technology
16 Stevinweg 1, Delft, The Netherlands, 2628 CN
17 Tel: +31 (0) 15 2787918; Fax: +31 (0) 15 2785767; Email: x.liu@tudelft.nl

19 **Panos Apostolidis**

20 Delft University of Technology
21 Stevinweg 1, Delft, The Netherlands, 2628 CN
22 Tel: +31 (0)616599128; Email: P.Apostolidis@tudelft.nl

24 **A. (Tom) Scarpas**

25 Delft University of Technology
26 Stevinweg 1, Delft, The Netherlands, 2628 CN
27 Tel: +31 (0)15 2784017; Email: A.Scarpas@tudelft.nl

29 **Liang He**

30 Chongqing Jiaotong University
31 No.66 Xuefu Rd., Nan'an Dist., Chongqing, China, 400074
32 Tel: +86 17782014964; Email: heliangf1@163.com

40 **Total Number of Words**

41	Words in abstract	=217	words
	Words in text:	=4090	words
	Words in references	=629	words
	Fig. & Tables (10x250)	=2500	words equivalent
	Total	=7436	words equivalent

42 Submitted for publication and presentation for the 96nd meeting of the Transportation Research Board

44 **ABSTRACT**

1 Low Temperature Asphalt (LTA) technologies are utilized in asphalt pavement industry to lower
2 energy demands and greenhouse gas emission during mixing and construction processes.
3 Although these technologies are currently available and hope to demonstrate similar performance
4 with Hot Mix Asphalt (HMA) mixes, LTA shows more sensitive than HMA to temperature
5 reduction during compaction and that will lead to inadequate compaction. Especially for Low
6 Temperature Porous Asphalt (LTPA) mixes, the quick reduction of mix temperature is the main
7 cause to poor pavements performance. The induction heating assisted compaction process appears
8 to be an effective way to ameliorate compaction issues and to improve the compactability at lower
9 temperatures. To design this process for LTA mixes, a numerical approach of combining the finite
10 and the discrete element methods is presented in this paper. Porous asphalt concrete was the
11 selected study material. The simulation process was divided into three steps: (i) temperature field
12 prediction during induction heating, (ii) adjustment of asphalt mortar parameters and (iii) asphalt
13 pavement compaction analysis. The effect of induction heating to asphalt compaction
14 effectiveness, the tendency of mix density changing along with the increase of compactor passes
15 and the influence of temperature on compaction at different locations in pavement were studied
16 and discussed as well.

17

18 *Keywords:* Low temperature asphalt, Induction heating, Compaction, Porous asphalt, DEM, FEM

19

1. INTRODUCTION

Asphalt concrete is a combination of asphalt binder, aggregates and filler particles. The aggregates and the binder act as structural skeleton and glue of the mix, respectively. The conventional asphalt mixes are produced and compacted at temperatures higher than 150 °C, because viscosity of asphalt binder impedes its workability at ambient temperature. However, working with mixes at such high temperatures greenhouse gas emissions and fumes are produced.

Considering the fact that the global asphalt industry is constantly looking for technological solutions to lower the energy demands and to reduce emissions, the utilization of technologies which reduce the mixing and the placement temperatures of asphalt pavements are under evaluation. These technologies are named Low Temperature Asphalt (LTA) (1-3). LTA materials refer to asphalt concrete mixes that are produced at temperatures approximately 30°C lower (or more) than temperatures typically used in the production of Hot Mix Asphalt (HMA).

There are important environmental and health benefits associated with lower production temperatures including lower fuel consumption, greenhouse gas emissions and reduced exposure of workers to asphalt fumes. Lower production temperatures can also potentially improve pavement performance by reducing asphalt binder aging, providing added time to mix compaction and allowing improved compaction during cold weather paving conditions.

A lot of effort spent worldwide and in the Netherlands on developing new materials and design specifications for durable Porous Asphalt (PA) pavement layers (5, 7, 9). Porous Asphalt (PA) mixes are mainly used as surface courses (4-6) and it is well-known that these mixes have been developed as a material solution to increase the skid resistance as well as to reduce splash during a rainstorm. Typically an asphalt surface layer is placed which has high air-void contents to absorb tire-pavement noise and good riding smoothness to reduce vehicle vibration related noise. Factors, such as aggregate characteristics, mix design, construction variables and environment play crucial role in the performance of PAs.

Several LTA processes are currently available for producing PAs. Their goal is to produce mixes with similar strength, durability and performance characteristics as HMAs using substantially reduced production temperatures. In view of this, PA is taken as an example in this research to study the construction process of low temperature porous asphalt pavement, and thus named LTPA hereinafter.

1.1 Compaction of LTPA Mixes

The compaction process of PAs differs from the conventional dense-graded mixes which involves both static steel wheel rollers and pneumatic-tired rollers (8). PAs are typically compacted only by a static steel roller with few passes over the surface (9, 10). However, serious problem of PAs compaction process is the aggregate segregation during laying down and the quick reduction of laying temperature, when the continuity of material supply to the construction site is irregular (11). The aggregate segregation causes unevenness in asphalt pavement surface and texture, while the rapid temperature reduction mainly causes inadequate compaction. All the beforementioned lead to poor PAs performance.

Asphalt compaction enhances interlocking of the aggregate-sized particles which increase the internal friction of the mix and this, in turn, provides a material with adequate stiffness and strength. However, inadequate compaction results in low mix density, high air-void content and reduction of mix fatigue life (9). Moreover, temperature is important factor for mix compaction. As temperature drops, the viscosity of asphalt mix is increased and hence coated aggregate mobilization reduction will result to diminished air-void content of mix and the time required to obtain the same degree of compaction increases.(9, 12).

1.2 Induction Heating as LTPA Compaction Assisted Technology

Induction heating (IH) is a technique very recently introduced into asphalt technology. Researchers at TU Delft were the first to explore the utilization of IH for healing of asphalt mixes (13-16). When an alternating electrical current is applied across an induction coil, an alternating magnetic field is developed. If the coil is placed in the vicinity of a material with inductive particles (e.g. asphalt including inductive fibres and/or filler-sized particles), then eddy currents are induced in the particles and heat is generated by the Joule's law. The heat generated by induction increases the temperature of the mix and enables healing of the micro-cracks by local melting of binder.

Asphalt IH is still a topic under investigation; nevertheless, the results are encouraging to expand the use of this technology to other asphalt applications. One such application is the utilization of induction technology to improve the compaction process of LTPAs. In this paper, a continuous IH-compaction process which consists of a continuously moving induction coil system and a roller compactor is presented, **Fig. 1**.

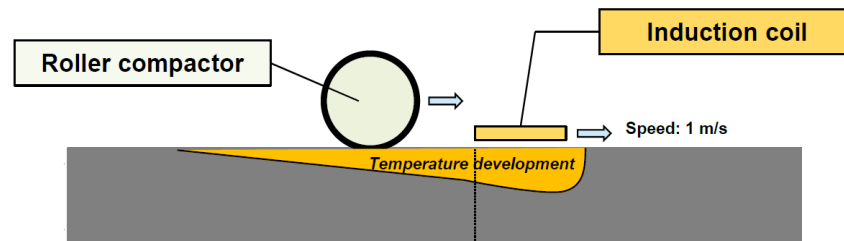


FIGURE 1 IH-compaction process

2. OBJECTIVES

In order to design the novel continuous IH-compaction process of LTPA mixes, Finite Element Method (FEM) and Discrete Element Method (DEM) were employed in this investigation to simulate IH assisted compaction process. Particularly, COMSOL multi-physics FEM and PFC3D DEM software were utilized in the study. The analyses have been divided into three sequential steps: (i) prediction of temperature field during IH, (ii) adjustment of the material parameters of asphalt mortar and (iii) execution of the corresponding compaction analysis, with main objectives:

- i. To demonstrate the impact of induction technology on the heat generation on the pavement surface by coupling and solving electromagnetic and heat transfer phenomena under a continuously travelling induction coil.
- ii. To simulate the compaction process with discrete element method and to predict the effect of induction technology on this process in different compaction environments.

3. MODELING OF INDUCTION HEATING ASSISTED COMPACTION PROCESS

3.1 Finite Element Modelling of Asphalt Induction Heating

Multi-physics modelling of electromagnetic heating phenomena provides a quick framework of analysis, especially suited for the study of complex composite materials such as asphalt mixes. For this reason, the focus is on the development of a computational approach to model IH pavements systems with continuously moving coils. COMSOL Multi-physics FEM software is used to

1 simulate a three-dimensional induction system of a single-turn coil and an inductive pavement
2 layer in this paper.

3 **Material selection and operational conditions**

4 An asphalt pavement and the air domain above the pavement surface were designed in such a way
5 that the induction coils were located in the centre. To simplify the response of the heated material,
6 it was assumed to be a homogeneous continuum medium with isotropic properties. The values of
7 the effective properties of inductive asphalt pavement were considered to be 1 for magnetic
8 permeability, 1 S/m for electrical conductivity, 6 for electrical permittivity, 1 W/(mK) for thermal
9 conductivity and 920 J/(KgK) for heat capacity (16). About the induction coil, copper was the
10 selected material in this analysis.

11 The IH model simulates both the magnetic field flux distribution around the induction coil,
12 through the asphalt pavement layer and the thermal behaviour of inductive asphalt layer. For more
13 details about the multi-physical phenomena of IH see (16). Furthermore, IH involves several
14 design and operational factors. However, analysis has been carried out under certain conditions.
15 Two travelling single-turn coils were utilized with 0.01 m of height and 0.2 m of width. The
16 selected operational conditions for this IH analysis were 70 kHz and 4 kV at 20 °C considering the
17 convenient induction examination at room temperature. The temperature development was studied
18 with the same speed as the moving speed of roller compactor of 1 m/s (~ 3.6 km/h).

19 **3.2 Discrete Element Modelling of Asphalt Compaction**

20 The DEM modelling is a computational approach in which the discontinuous materials are
21 modelled as individual elements and it was introduced by Cundall et al. (17, 18). This approach
22 allows the simulation of complex and heterogeneous materials taking into account the contacts and
23 the interaction of particles within the aggregate skeleton.

24 **Material selection**

25 During the years, Dutch authorities and contractors have tried to address the issues of surface
26 pavement layers by developing PA mixes. Two characteristic examples of surface layers
27 commonly used in the Netherlands are: (i) the Two Layer PA with 0/16 and 0/8 aggregate matrix in
28 the bottom and top layer, respectively, and (ii) the Single Layer PA of 0/16 aggregate matrix (10),
29 which was used in this study, **Table 1**. In the PA 0/16 aggregate gradation, steel slag particles (finer
30 fraction 2mm) were added as low cost inductive agents by replacing mineral aggregates of the
31 same fraction.

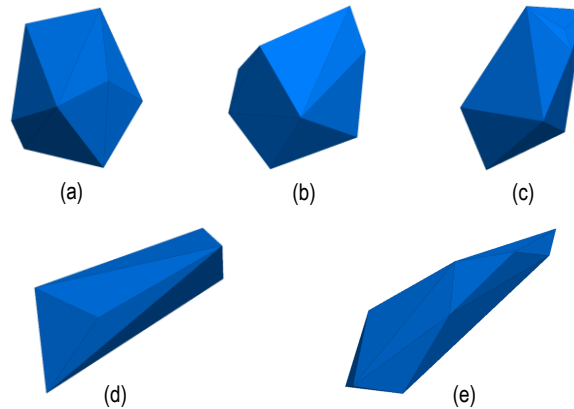
32 **TABLE 1 Aggregate gradation of PA 0/16 mix**

Sieving size (mm)	22.4-16.0	16.0-11.2	11.2-8.0	8.0-5.6	5.6-2.0	2.0-0.063	<0.063
Cum. Ret. (%)	4	25	57	80	85	95.5	100
% ret. by weight	4	21	32	23	5	10.5	4.5

33 **Micro-mechanical modelling of asphalt mix**

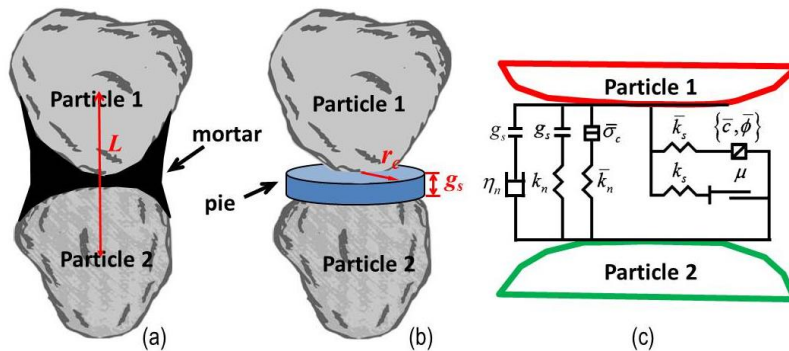
34 To simplify the micro-mechanical modelling of LTPAs, the mix was divided into three different
35 individual constituents; (i) coarse aggregate particles larger than 2.0 mm, (ii) asphalt mortar and
36 (iii) air-voids. Considering that the shape of the coarse aggregates, which form the aggregate
37 skeleton in the mix, have an major impact on the mix compaction, five different particles with
38 complex geometries, **Fig. 2**, were developed to compose the PA 0/16 material. The shape of each
39 aggregate particle was randomly chosen from these five shapes. The values of $L:W:H$ denotes the
40
41
42
43
44
45

1 ratio of particle's length, width and height, respectively, and they were used to control the flatness
 2 and elongation of particles, **Fig. 2**.
 3



4
 5 **FIGURE 2** Generated coarse aggregate particles: (a&b) $L:W:H=1:1:1$, (c&d) $L:W:H=1:0.8:0.6$ and
 6 (e) $L:W:H=1:0.5:0.25$
 7

8 For the DEM modelling, asphalt mortar (i.e., asphalt binder, mineral filler and fine sand), which
 9 was added as the bond between the generated coarse aggregate particles in analyses, was
 10 considered to be continuum and homogeneous. The bond was envisioned as a *pie* made by many
 11 elastic springs lying on the contact plane and centred at the contact point of two particles, **Fig.3**.
 12 When the *pie* is bonded, it can resist the tensile force and the relative rotation moment until the
 13 tensile strength or shear strength limit of the spring is exceeded. After the break of contact bonds,
 14 only compressive forces are active.
 15



16
 17 **FIGURE 3** Schematic of contact conditions between the coarse aggregate particles: (a) asphalt
 18 mortar, (b) pie-shaped bond, and (c) physical model of bond
 19

20 Due to the fact that when two aggregates covered by asphalt mortar they are easily glued
 21 together during moving, the broken bond may be re-glued again when the particles are close
 22 enough. This is the biggest different between compaction simulation and the common mechanical
 23 analysis for asphalt mix. This mechanism can be realized through continually judging and
 24 generating new bonds when necessary but keeping the state of old bonds unchanged during the
 25 cycle.

26 The pie shaped bond model is determined by five key parameters related to asphalt mortar.
 27 These parameters are: (i) the normal stiffness \bar{k}_n , (ii) the shear stiffness \bar{k}_s , (iii) the tensile strength

1 $\bar{\sigma}_c$, (iv) the shear strength $\bar{\tau}_c$ (calculated by cohesion c and angle of internal friction ϕ) and (v) the
 2 pie radius r_c . Also, parameter such as the gap between the particles g_s , the viscosity of contact η_n
 3 and the friction of contact μ should be taken into account for the model development, **Fig. 3**. The
 4 particle contact behaviour of compression is governed by Kelvin-Voigt constitutive laws and that
 5 of tension is determined by Mohr-Coulomb failure criterion.

7 **Model parameters determination**

8 The before mentioned five parameters have a great influence on the degree of asphalt compaction
 9 and are determined by the mix temperature. However, the compactability of mix, which is
 10 influenced by the temperature as well, is determined by the air-void content. Research (19) showed
 11 that the air-void content is linearly related to the coordination number. The coordination number of
 12 a particle is defined as the total number of particles which are in contact with. In this paper, the
 13 air-void content of mix was changed by compressing the same pavement DEM model and the
 14 relationship was obtained as shown in **Fig. 4(a)**,
 15

$$n = n_0 + A\bar{n}_c \quad (1)$$

16 where n is the air-void content. \bar{n}_c is the average coordination number of aggregates. n_0 and A are
 17 coefficient.

19 *Stiffness of asphalt mortar*

20 The relationship of dynamic module of asphalt mortar under different temperatures was
 21 investigated by Fernandes et. al. (20) and it expressed as shown in **Eq. 2**
 22

$$E^* = E_0 e^{-\alpha T} \quad (2)$$

23 where E^* is the dynamic modulus of the mortar (MPa), T is the temperature, E_0 and α are the
 24 complex parameters.

26 In this bond model, asphalt mortar can be envisaged as a cluster of spring. Dynamic modulus
 27 was replaced by the stiffness and the relation is given in **Eq. 3**
 28

$$K = \frac{E^*}{L} \quad (3)$$

29 where K is the stiffness of bond (MPa/m), L is the distance of centroid of two particles that are
 30 bonded. This relationship shows that the value of stiffness is reduced when two particles moving
 31 away and by keeping dynamic modulus constant.

33 In this research, dynamic modulus of LTPA mortar was assumed to obey the curve shown in
 34 **Fig. 4(b)** and the stiffness in normal direction was kept same as that in shear direction.

36 *Strength of asphalt mortar*

37 Since the asphalt mortar is assumed as a viscoelastic material, a peak value of stress and permitted
 38 strain exist. When a bond exceeds any one of these limits, the bond can be treated as broken and the
 39 rheological property of mortar are easily reflected. The tensile and shear strength of asphalt mortar
 40 has been investigated and the obtained results demonstrate that that the strength is exponentially
 41 related to the temperature (21-23) (**Fig. 4(c) & Eq. 4**)

1

$$\sigma_c = \sigma_0 e^{-\beta T} \quad (4)$$

2

3 where σ_c is the tensile strength, σ_0 and β are the corresponding parameters.

4

5 The elastic energy stored in the springs of the bond can't be released, as is obviously not
6 consistent with the purpose of simulation. Therefore, a critical strain should be applied onto the
7 model. Then the effective strength of mortar can be written as

7

$$\bar{\sigma}_c = \min(\sigma_c, \bar{\epsilon}_r E^*) \quad (5)$$

8

9 where $\bar{\sigma}_c$ is the effective strength and $\bar{\epsilon}_r$ is the critical strain. In this research, $\bar{\epsilon}_r$ is given by **Eq. 6**

9

$$\bar{\epsilon}_r = 0.017 e^{-0.018 T} \quad (6)$$

10

11 *Angle of Internal Friction*

12

13 Since the failure mode of asphalt mortar was controlled by the Mohr-Coulomb strength criterion,
14 the shear strength of the mortar will be determined by the normal stress σ , the cohesion c and the
15 internal friction angle φ . Herein, only the angle of internal friction is discussed, which is
16 influenced by the temperature and the compactability of the mix (23,24). This parameter refers not
17 only to the attribution of asphalt mortar but also to the whole interaction of contacted particles. In
18 Hopkins' research (23), the angle of internal friction is given by **Eq. 7** as function of temperature

18

$$\varphi_t = 20.7 + \frac{6.792}{(1.8T + 32)} + \frac{494.466}{(1.8T + 32)^2} \quad (7)$$

19

20 As shown in Tinoco's report (24), the internal friction angle reduces along with increase of air-void
21 content of mix. The obtained data is listed in **Table 2**. Based on these results, the angle was
22 determined by the following function

23

$$\varphi = \gamma_n \cdot \varphi_t = \gamma_{nc} \cdot \varphi_t \quad (8)$$

24

25 where φ is the internal friction angle of bond, φ_t is the friction angle based on the temperature, γ_n is
26 the coefficient caused by the variation of air-void content and γ_{nc} is corresponding expression of γ_n
27 in the form of coordinate number, which is given by the **Table 2** as well.

28

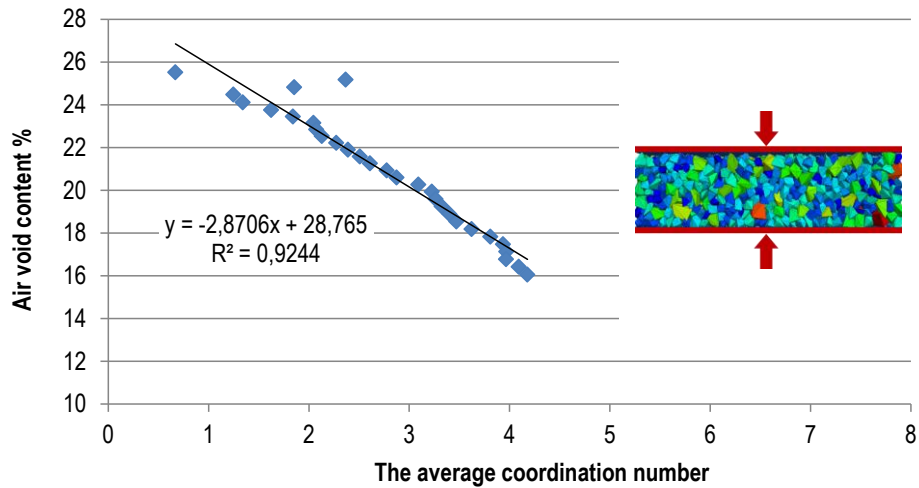
29 **TABLE 2 Internal friction angle as function of air void content and the used coefficient γ_{nc}**

30

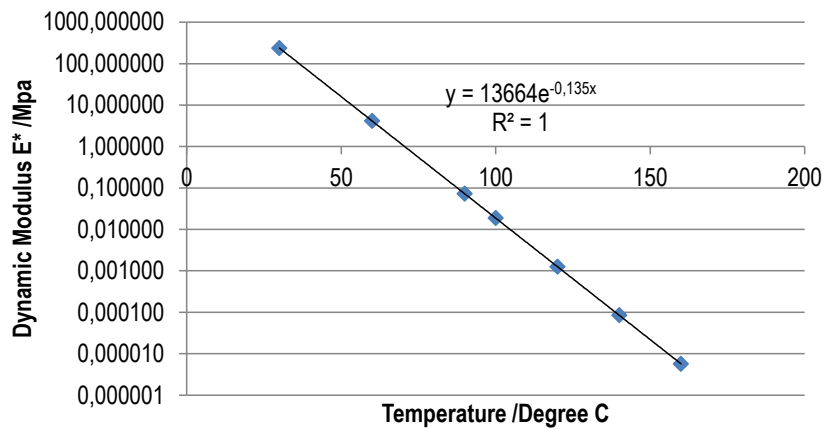
Air void content (%)	22	21.5	21	20.5	20	19	18	17			
Angle of internal friction φ (°)	47.5	51.0	52.0	52.5	52.7	53.0	53.4	53.5			
The coordination number	0	1	2	3	4	5	6	7	8	9	10
γ_{nc}	0.000	0.543	0.826	0.913	0.946	0.961	0.967	0.978	0.989	0.996	1.000

31

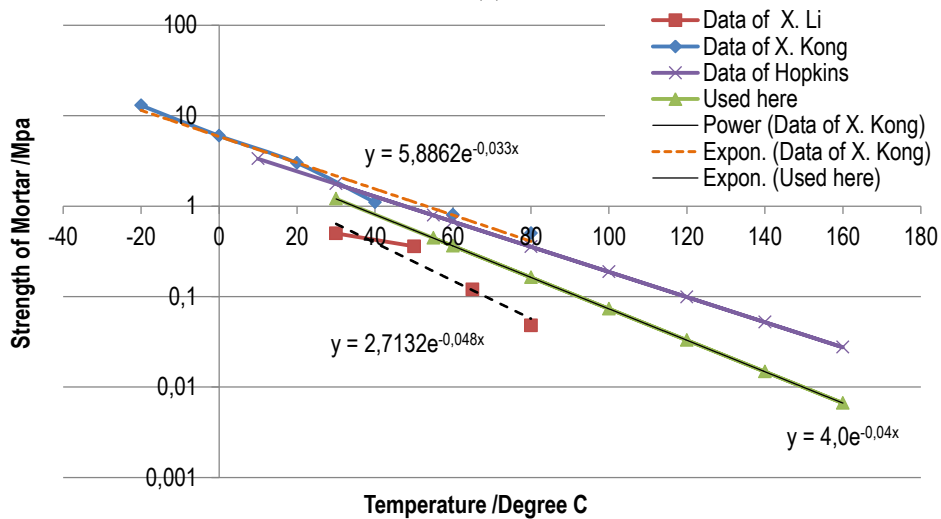
32



(a)



(b)



(c)

1
2 **FIGURE 4 Determination of model parameters: (a) relationship between air-void content and the**
3 **average coordination number, (b) dynamic modulus of LTPA mortar, (c) strength curves of asphalt**
4 **mortar from literature**

1 *Bond Radius*

2 The bond radius greatly influences the bond damage in the asphalt mortar. An easy way to obtain
3 this parameter is to calculate it through the total effective volume of the asphalt mortar. Moreover,
4 assuming that the bond radius ratio ζ is defined as the ratio of bond radius r_c to the minimal radius
5 \bar{R} of equivalent sphere with same volume as the bonded particles. The total effective volume of
6 mortar and the radius ratio ζ can be estimated by **Eq. 9 & 10**.

$$7 \quad V_m = \sum_{i=1}^{N_b} [\pi(\zeta\bar{R}_i)^2 \cdot L] = \zeta^2\pi \sum_{i=1}^{N_b} [\bar{R}_i^2 \cdot L] \quad (9)$$

$$8 \quad \zeta = \sqrt{\frac{V_m}{\pi \sum_{i=1}^{N_b} [\bar{R}_i^2 \cdot L]}} \quad (10)$$

9
10 where V_m is the total volume of mortar, N_b is the total number of bond at a given time and L is the
11 distance of the two bonded particles, as same as **Eq. 3**.

12 When asphalt mortar becomes denser, the bond radius obviously becomes larger. However, it is
13 difficult to give an explicit equation between them. Here, L is assumed to be lineally related to the
14 air-void content within a short content range. Thus, distance L can be described using coordination
15 number as

$$16 \quad L = L_0 + bn_c \quad (11)$$

17
18 where n_c is the a particle's coordination number. L_0 and b are the corresponding coefficients.

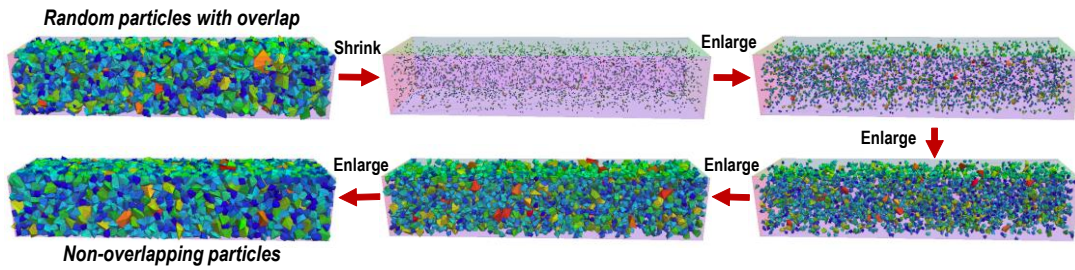
19 Also, by substituting **Eq. 11** to **Eq. 10**, **Eq. 12** is formulated

$$20 \quad \varepsilon^2 = 1 + sn_c \quad (12)$$

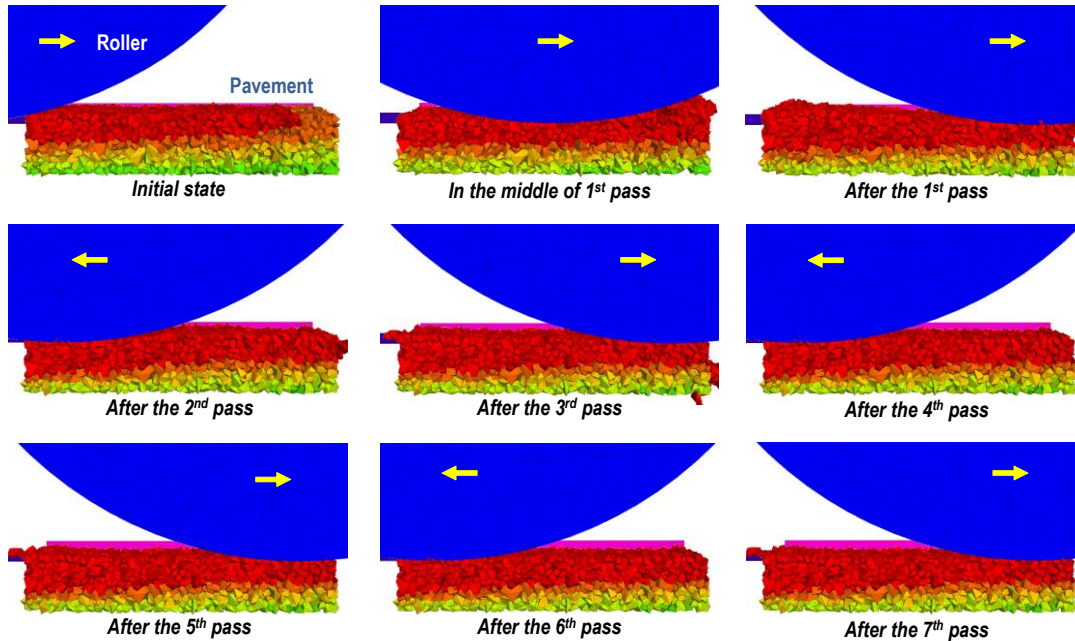
21
22 where ε is the enlargement multiplier of bond radius ratio ζ and s is the coefficient related to
23 coordination number.

24 25 **Pavement model creation and compaction method**

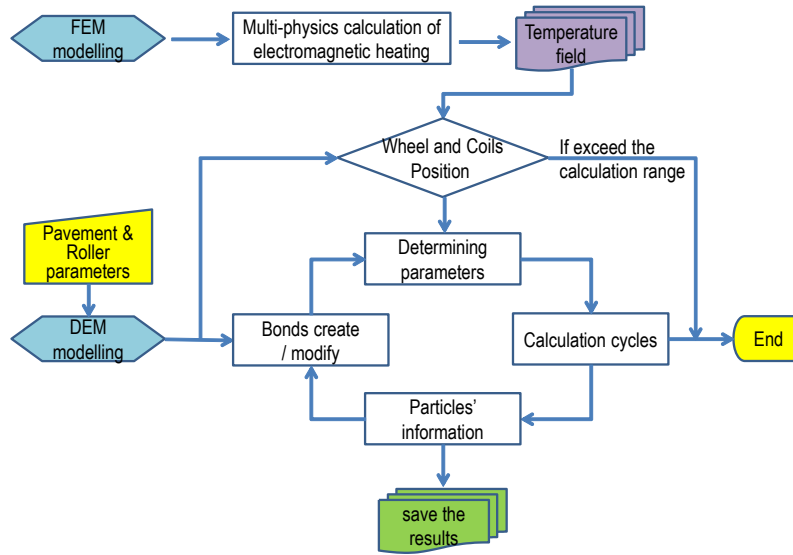
26 Before simulating the compaction process of LTPA, a new models have to be created. Since there
27 is not a mature approach to create such models directly with required air-void content, in order to
28 make full use of the DEM mechanics and to keep the gradation distribution of mix unchanged, the
29 following procedure has been ensued: (i) calculation of the total volume of particles according to
30 the pavement model size and the required/initial air-void content; (ii) calculation of the particle
31 numbers of different size on the basis of the mix gradation; (iii) random generation of these
32 particles (where the particles may overlap each other); (iv) shrinkage of all the particles by 50
33 times for example; and (v) enlargement of the particles step-by-step (between each steps, the
34 overlaps were eliminated by DEM simulation). If each particle enlarges $\sqrt[10]{50}$ times per step, all
35 the particles will change back to the original size again after 10 steps, and meanwhile, the air-void
36 content of pavement model will reach the value that was set, **Fig. 5(a)**. Note that, in this process,
37 pie shaped bond model will be unnecessary and elastic contact model will be enough.



(a)



(b)



(c)

1 **FIGURE 5 Simulation process of LTPA: (a) pavement model generation process, (b) pavement**
 2 **compaction process (due to space limitations, only part of the wheel is retained in the picture), and**
 3 **(c) schematic flow diagram of this coupling methodology**
 4

The compaction procedure is achieved by an rigid wheel (roller wheel), which rolls on the pavement model with a given weight. When the roller moves close to the border of the pavement model, one pass is finished. Then the roller will go back its original location and repeat this procedure until to the end, see **Fig. 5(b)**.

A schematic flow diagram of the coupling methodology is demonstrated in **Fig. 5(c)**, which explains how the DEM combines with FEM results to simulate induction assisted compaction.

4. RESULTS AND MAIN FINDINGS

Based on the aforementioned methodology, some main findings of this study are showing in the flowings.

4.1 Effect of Induction Heating on Temperature Development

The temperature development and the heat pattern of inductive LTPA pavement layer was predicted and the results are shown in **Fig. 6**. The continuous moving induction system of two single-turn coils with a speed of 1m/s generated heat at the surface of asphalt layer of 20°C after 120 seconds of induction. In **Fig. 6(a)**, the contour lines show the evolution of the temperature gradient at the asphalt surface and the maximum generated temperatures appear close to the coil's gates where the concentration of magnetic fields is higher.

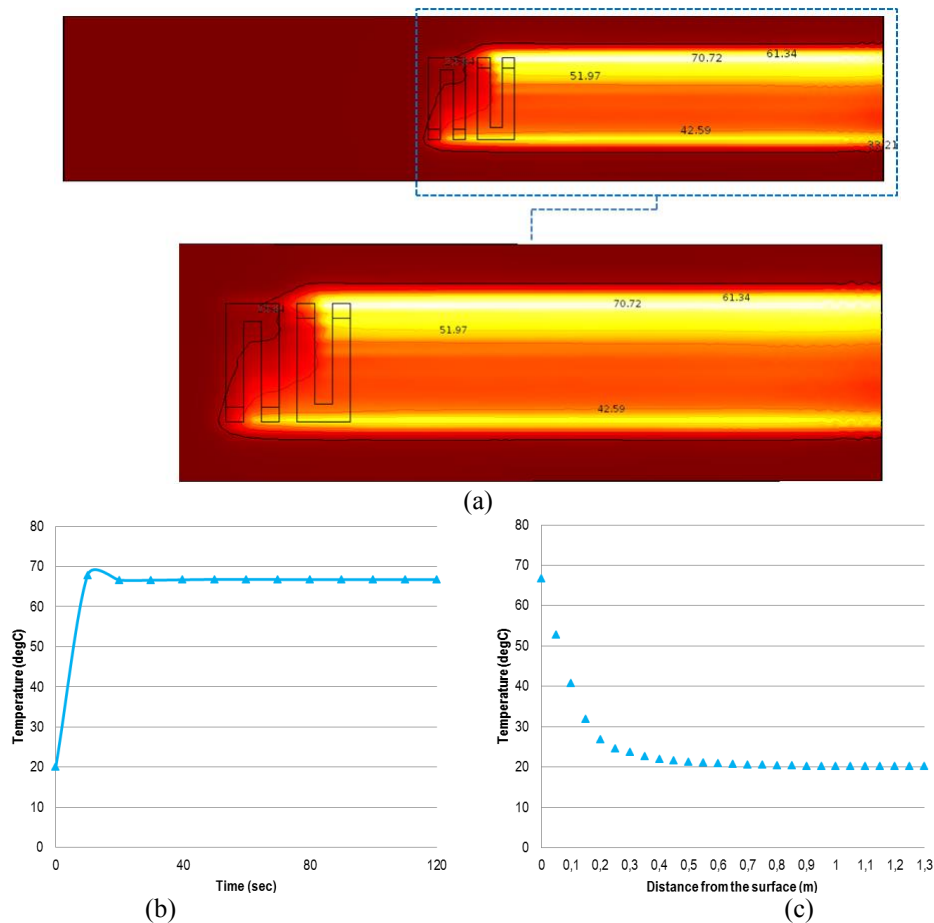


FIGURE 6 FEM results of induction heating on pavement: (a) thermal field distribution at pavement surface, (b) surface temperature development of pavement and (c) temperature distribution in pavement after 120 seconds of induction

1 However, apart from the highest reached temperature of the surface of asphalt layer, increased IH
 2 efficiency (temperature after 120 seconds of induction) resulted also within the asphalt layer, **Fig.**
 3 **6(b)**. The temperature distribution from the top to the bottom of the inductive asphalt layer is
 4 illustrated in **Fig. 6(c)**. This distribution inside the layer shows the advantage of utilizing the
 5 induction technology as heating technique in order to minimize temperature reduction phenomena
 6 during asphalt compaction. Thus, the viscosity of asphalt mixes can be maintained increasing thus
 7 the time required for adequate compaction under low temperature conditions.

9 **4.2 Effect of Induction Heating on LTPA Compaction Process**

10 The asphalt pavement compaction model has been created by taking into account the effect of IH
 11 and its generated temperature field, which was calculated in the previous subchapter. It was
 12 assumed that the generated heat for asphalt pavements of initial temperature 20 °C is also valid for
 13 higher initial temperatures. All the parameters of asphalt compaction process were shown in **Table**
 14 **3**.

16 **TABLE 3 Parameters used in DEM analysis**

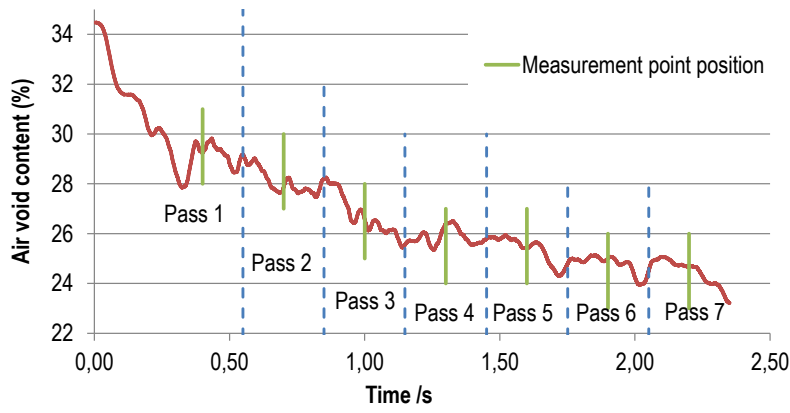
Parameters	Values
<i>Pavement model</i>	
model size	50cm(length) × 50cm(width) × 8cm(thickness)
particles size	2mm-22.4mm (PA 0/16)
<i>Roller Parameter</i>	
wheel size	100cm(diameter) × 200cm(width)
wheel weight	5 tons (one wheel)
<i>Mortar parameters</i>	
Air-void content estimated	$n = -2.8706 + 28.765\bar{n}_c$
dynamic modulus(MPa)	$E^* = 13664.0e^{-0.135T}$
critical strain	$\bar{\epsilon}_r = 0.017e^{-0.018T}$
effective strength (MPa)	$\bar{\sigma}_c = 232.29e^{-0.153T}$
initial bond radius ratio	$\zeta_0 = 0.06$
enlargement multiplier of bond radius	$\epsilon = \sqrt{1 + 0.06n_c}$

18 Based on the DEM analysis, the results of asphalt compactability or air-void content in relation to
 19 the roller passes are shown in **Fig. 7**. Four cases were considered:
 20

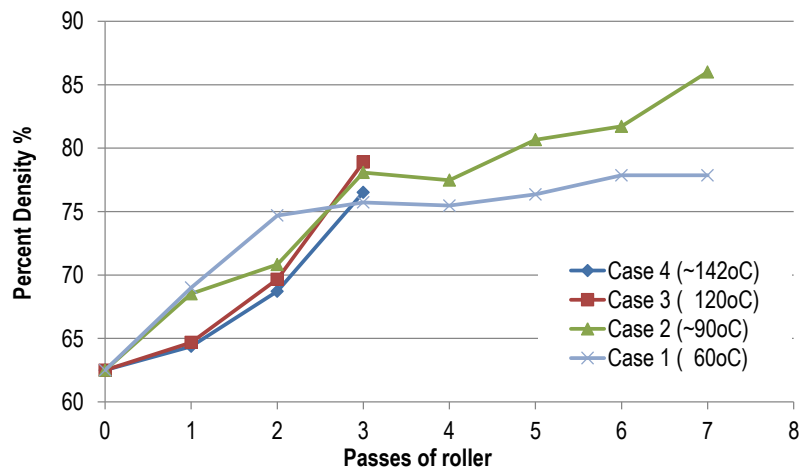
- 21 Case 1: Mix temperature $T_0=60^\circ\text{C}$ without IH
 22 Case 2: Mix temperature $T_0=60^\circ\text{C}$ with IH (surface temperature of $T_f \approx 90^\circ\text{C}$)
 23 Case 3: Mix temperature $T_0=120^\circ\text{C}$ without IH.
 24 Case 4: Mix temperature $T_0=120^\circ\text{C}$ with IH (surface temperature of $T_f \approx 142^\circ\text{C}$)

25 From the **Fig. 7(a)**, it was found that during the first pass (initial compaction), the air-void content
 26 fluctuated dramatically and the mix easily flown. If taking the studied point as reference, when the
 27 compactor comes close to it, the mix air-void content declines because of aggregates' pushing
 28 movement. While when the roller moves to the right above of the point, many bonds are broken
 29 caused by tensile stress and the air-void content shows a slight increase. When the roller moves off
 30 this point, the air-void content goes down again and the mix are re-compacted. With passes
 31 increase, the air-void content continually declines, while fluctuation start to be stable and the

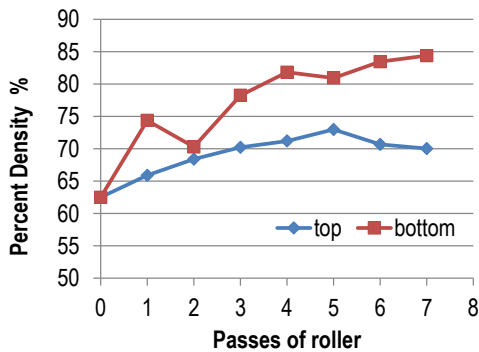
1 variation amplitude of porosity reduces.
 2



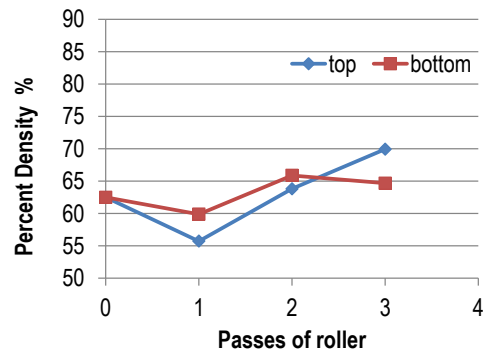
(a)



(b)



(c)



(d)

3 **FIGURE 7 Simulation results of DEM: (a) the air-void content changes as passes increase at 60°C**
 4 **with induction heating, (b) comparison of compaction effect for different case, (c) percent density in**
 5 **different depth for (c) case 2 (~90 °C) and (d) case 4 (~142 °C)**

6
 7 **Fig. 7(b)** shows that the entire compaction process can be divided into two distinct stages: early
 8 stage (passes <3) and late stage (passes >3). Comparing with the Case 1 (without IH) and Case 2
 9 (with IH), it was found that the air-void content was lower in early-stage IH-compaction process
 10 than the asphalt compaction process without IH during at the same stage. For both cases, the final

1 void content of early was higher than that of late stage. Higher temperatures do not always increase
2 the density of the material but also increase the liquidity of particles and subsequently the bad
3 compactability of the mix. The IH operates efficiently in the later stage after the density reaches a
4 certain value, rather than at the very beginning. Moreover the effect of IH on asphalt compaction
5 process is not obvious at higher temperatures.

6 **Fig. 7(c&d)** demonstrates the change of air-void content in different depths (top and bottom)
7 with increasing the roller passes. These curves show that the air-void content on the bottom of
8 asphalt layer changed considerably than on the top at lower temperature. That might be caused by
9 the change of stiffness balance due to IH. The stiffness of top of asphalt was reduced when was
10 heated. On the contrary, for higher temperatures, the difference of density in different layer is not
11 distinct because the balance of stiffness hardly changed.

12

13 **5. CONCLUSIONS AND RECOMMENDATIONS**

14 This paper introduced a discrete element method combined with finite element method to simulate
15 the compaction process of low temperature asphalt pavement assisted by induction heating. Based
16 on the current study, following conclusions can be made:

- 17 (1) Multi-physics modelling of electromagnetic heating phenomena provides a quick method to
18 model induction heating pavements systems with continuously moving coils, which can
19 effectively solve the problem of multi-physics simulation faced on the DEM.
- 20 (2) The key point of the DEM modelling approach introduced in this paper is to dynamically and
21 continuously change the microstructure parameters of asphalt mortar according to the
22 moving temperature field from the induction heating in FEM. This method proved to be
23 effective and encouraged through the example cases.
- 24 (3) Based on the analyses, the asphalt compaction process can be divided into two stages: early
25 and late stage. In the early stage, the density remained unchanged of the mix compacted with
26 induction technology. In the late stage, the final density with heating will be larger than the
27 compaction process without induction. The induction heating operates better at lower mix
28 temperatures.
- 29 (4) The induction heating mostly influences the balance of stiffness at different pavement depths.
30 For high temperature mix, the effect of induction is small. However, for lower temperatures,
31 the heating always leads to higher density at the bottom of pavement than at top.

32 Although the objective of this paper was mainly to discuss the induction heating assisted
33 compaction technology and the developed numerical approach, it is very necessary to carry out
34 lab-scale tests to obtain the required parameters in further research and then to verify the results of
35 these analyses.

36

37 **REFERENCES**

- 38 1. CROW, *Low Temperature Asphalt for a Sustainable Pavement*, ISBN-978 90 6628 613 9,
39 CROW Publication 319, the Netherlands.
- 40 2. European Asphalt Pavement Association. *The Use of Warm Mix Asphalt*. EAPA-Position
41 Paper, 2014.
- 42 3. Hanz, A., A. F. Faheem, E. Mahmoud, H.U. Bahia. Measuring Effects of Warm-Mix
43 Additives: Using a Newly Developed Asphalt Binder Lubricity Test for DSR.
44 *Transportation Research Record: Journal of the Transportation Research Board, No. 2180*,
45 Washington, D.C., 2010, pp.85-92
- 46 4. Kandhal, P.S., R.B. Mallick. Open-Graded Friction Course: State of the Practice.
47 *Transportation Research Circular*, 1998.

- 1 5. Smith, H.A. Performance Characteristics of Open-Graded Friction Courses. In *NCHRP*
2 *Synthesis of Highway Practice, No. 180*, Transportation Research Board, National Research
3 Council, Washington, D.C., 1992.
- 4 6. Hagos, E.T. *The Effect of Aging on Binder Properties of Porous Asphalt Concrete*. PhD
5 Thesis, TU Delft, 2008.
- 6 7. Van der Zwan, T. Goeman, H.J. Gruis, J.H. Swart, R.H. Oldenburger. Porous Asphalt
7 Wearing Courses in the Netherlands: State of the Art. *Transportation Research Record, No.*
8 *1265*, TRB, Washington, D.C., 1990, pp. 95-110.
- 9 8. Austroads. *The Influence of Compaction on the Performance of Dense Graded Asphalt*.
10 Austroads Project TT1353, 2011, Austroads, Sydney, Australia.
- 11 9. Lu, Q., J.T. Harvey. Laboratory Evaluation of Open-Graded Asphalt Mixes with Small
12 Aggregates and Various Binders and Additives. *Transportation Research Record, No. 2209*,
13 Washington, D.C., 2011, pp. 61-69.
- 14 10. Lugo, A.E., A. Epps Martin, C.K. Estakhri, J.W. Button, C.J. Glover, S.H. Jung. Synthesis of
15 Current Practice on the Design, *Construction and Maintenance of Porous Friction Course*.
16 Technical Report. 0-5262-1, 2006, Texas Transportation Institute, Houston, TX.
- 17 11. Molenaar, A.A.A., A.J.J. Meeker, A. Miradi, T. van der Steen. Performance of Porous
18 Asphalt concrete. *Journal of the association of asphalt paving technologists*. Vol. 75, 2006.
- 19 12. Kragh, J., L. Goudert, U. Sandberg. OPTHINAL: Optimization of Thin Asphalt Layers.
20 ERA-NET Road, Final Report, Project No. VV 2009/40520, 2011.
- 21 13. Liu, Q., E. Schlangen, M. van de Ven. Induction Heating of Electrically Conductive Porous
22 Asphalt Concrete. *Transportation Research Record, No. 2305*, TRB, Washington,
23 D.C., 2012, pp. 95-101.
- 24 14. Apostolidis, P., X. Liu, A. Scarpas, C. Kasbergen, M.F.C. van de Ven. Advanced Evaluation
25 of Asphalt Mortar for Induction Healing Purposes. *Construction and Building Materials* 126,
26 2016, pp. 9-25.
- 27 15. Apostolidis, P., X. Liu, T. Scarpas, G. van Bochove, M. van de Ven. Advanced
28 Experimental Evaluation of Asphalt Mortar for Induction Healing Purposes. In
29 *Transportation Research Board 95th Annual Meeting, No.16-3780*, Washington D.C., 2016.
- 30 16. Apostolidis, P., X. Liu, T. Scarpas, M. van de Ven, G. van Bochove. Investigation of
31 Induction Heating in Asphalt Mortar: Numerical Approach. In *Transportation Research*
32 *Board 95th Annual Meeting, No. 16-3772*, Washington D.C., 2016.
- 33 17. Cundall, P.A. A Computer Model for Simulating Progressive, Large-scale Movements in
34 Block Rock Systems. *Proc. Symp. Int. Soc. Rock Mech*, 1971.
- 35 18. Cundall, P.A., Strack, O. D. A Discrete Numerical Model for Granular Assemblies.
36 *Geotechnique*, Vol.29, 1979, pp. 47-65.
- 37 19. Huang Q, Zhan M, Sheng J, et al. Numerical Method to Generate Granular Assembly with
38 any Desired Relative Density based on DEM, *Chinese Journal of Geotechnical Engineering*,
39 Vol. 37, no. 3, 2015, pp.537-543.
- 40 20. Fernandes M R S, Forte M M C, Leite L F M. Rheological Evaluation of Polymer-modified
41 Asphalt Binders. *Materials research*, 2008, Vol.11, No.3, pp. 381-386.
- 42 21. Li X, Zhang X, Wang S. Study of High Temperature Performance of Asphalt Mastic Based
43 on Dynamic Viscoelastic Mechanics. *Journal of Highway and Transportation Research and*
44 *Development*, 2007, Vol. 2, No.2, pp.16-20.
- 45 22. Kong X, Liu Y, Zhang Y, et al. Influences of Temperature on Mechanical Properties of
46 Cement Asphalt Mortars. *Materials and Structures*, 2014, Vol.47, No.1-2, pp. 285-292.
- 47 23. Hopkins T C, Sun L, Slepak M E. *Bearing Capacity Analysis and Design of Highway Base*
48 *Materials Reinforced with Geofabrics*. 2005.
- 49 24. Tinoco FH, Handy RL, Hoover JM. *Void Ratio and Shear Strength of Two Compacted*
50 *Crushed Stones*. 1965.